Activation phenotype, rather than central– or effector–memory phenotype, predicts the recall efficacy of memory CD8$^+$ T cells

Hirokazu Hikono, Jacob E. Kohlmeier, Shiki Takamura, Susan T. Wittmer, Alan D. Roberts, and David L. Woodland

Trudeau Institute, Saranac Lake, NY 12983

The contributions of different subsets of memory CD8$^+$ T cells to recall responses at mucosal sites of infection are poorly understood. Here, we analyzed the CD8$^+$ T cell recall responses to respiratory virus infection in mice and demonstrate that activation markers, such as CD27 and CD43, define three distinct subpopulations of memory CD8$^+$ T cells that differ in their capacities to mount recall responses. These subpopulations are distinct from effector– and central–memory subsets, coordinately express other markers associated with activation status, including CXCR3, CD127, and killer cell lectin-like receptor G1, and are superior to CD62L in predicting the capacity of memory T cells to mediate recall responses. Furthermore, the capacity of vaccines to elicit these memory T cell subpopulations predicted the efficacy of the recall response. These findings extend our understanding of how recall responses are generated and suggest that activation and migration markers define distinct, and unrelated, characteristics of memory T cells.

CORRESPONDENCE
David L. Woodland:
dwoodland@trudeauinstitute.org

Abbreviations used: EID, egg infectious dose; KLRG1, killer cell lectin-like receptor G1; MLN, mediastinal lymph node; PD-1, programmed death-1.

A defining feature of the adaptive immune system is the capacity to "remember" past encounters with a pathogen and subsequently mount superior responses (recall responses) to a secondary challenge with the same, or related, pathogen (1). In the case of influenza and parainfluenza virus infections, it has been established that antigen-specific CD8$^+$ T cells elicited during a primary infection persist at high frequencies for years after clearance of the virus (2–4). These memory CD8$^+$ T cells are able to mediate recall responses that result in accelerated viral clearance and survival after challenge with an otherwise lethal dose of virus (5, 6). The enhanced responsiveness of antigen-specific memory CD8$^+$ T cells as compared with naive CD8$^+$ T cells is due to increased cell numbers, higher activation status, reduced stimulatory requirements, more rapid acquisition of effector functions, and altered homing patterns (1, 7, 8).

Memory CD8$^+$ T cells are heterogeneous in terms of phenotype, function, and anatomical distribution. This heterogeneity is thought to reflect the different functional characteristics and migratory properties of memory CD8$^+$ T cell subsets and has led to the paradigm that memory cells can be divided into two major subsets: central– and effector–memory T cells (2, 3, 6, 9–15). Central–memory T cells express high levels of CD62L and CCR7, which directs them to enter high endothelial venules and thereby localize predominantly in secondary lymphoid tissues. Effector–memory T cells express low levels of CD62L and CCR7 and tend to localize predominantly in nonlymphoid and peripheral tissues (15, 16). The different characteristics of central– and effector–memory CD8$^+$ T cells suggest that these cells play different roles in recall responses. However, the relative contributions of each subpopulation to the accumulation of fully activated effector cells during a recall response after secondary infection are unclear (17–19). One possibility is that effector–memory T cells that accumulate in peripheral sites such as the lung mediate early and nonsustained responses to the pathogenic challenge, whereas central–memory cells in secondary lymphoid organs mediate a late but sustained proliferative response to the challenge (20). However, studies on the capacities of effector– and central–memory cell subpopulations to mediate recall responses in vivo have been contradictory. Several groups have shown

H. Hikono and J.E. Kohlmeier contributed equally to this work.

H. Hikono's present address is National Institute of Animal Health, Tsukuba, Ibaraki 305-0856, Japan.

The online version of this article contains supplemental material.

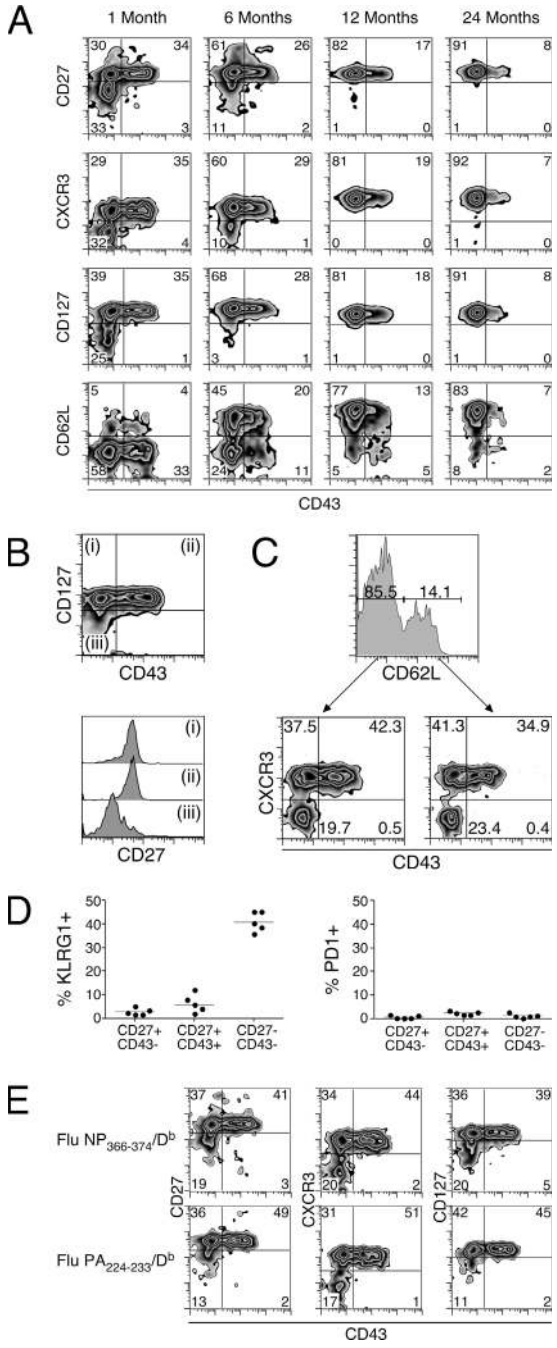

Figure 1. Memory CD8$^+$ T cells can be divided into three major subsets. (A) Splenocytes isolated at various times after infection were stained with Sendai $NP_{324-332}/K^b$ tetramer and monoclonal antibodies. The profiles are gated on tetramer$^+$/CD8$^+$ cells, and the numbers indicate the percentage of gated cells in each quadrant. Data are representative of six individual mice at 1 and 6 mo after infection, and three individual mice at 12 and 24 mo after infection. (B) Splenocytes isolated 1 mo after Sendai infection were stained as described in A and gated on tetramer$^+$/CD8$^+$cells. The top plot depicts the CD127 × CD43 profile of tetramer$^+$ cells, and the roman numerals correspond to the expression of CD27 (shown in the histograms below) within the indicated quadrant. (C) Splenocytes isolated 1 mo after Sendai virus infection were stained as described for A and gated on tetramer$^+$/CD8$^+$ cells. CXCR3 × CD43 profiles were then determined on either CD62L^{lo} or CD62L^{hi} cells. Data are from the same staining experiment as in A. (D) Splenocytes isolated 1 mo after Sendai virus infection were stained with $NP_{324-332}/K^b$ tetramer and monoclonal antibodies. Data show the percentage of KLRG1$^+$ or PD1$^+$ cells among tetramer$^+$/CD8$^+$ cells that had been subgated into CD27^{hi}/CD43^{lo}, CD27^{hi}/CD43^{hi}, and CD27^{lo}/CD43^{lo} subpopulations. (E) Splenocytes isolated 1 mo after intranasal x31 influenza virus infection were stained with either Flu $NP_{366-374}/D^b$ tetramer or Flu $PA_{224-233}/D^b$ tetramer and monoclonal antibodies as described in A. The data in each subpanel are gated on either Flu $NP_{366-374}/D^b$ tetramer$^+$/CD8$^+$ cells (top) or Flu $PA_{224-233}/D^b$ tetramer$^+$/CD8$^+$ cells (bottom), and the numbers represent the percentage of cells in each quadrant. The data are representative of three independent experiments.

that central–memory T cells dominate recall responses to pathogens that mediate systemic infections, although this does not necessarily correlate with protective efficacy (16, 21–25). Conversely, other studies have shown that effector–memory CD8$^+$ T cells can contribute equally to, or even dominate, recall responses (26, 27). We have used a dual adoptive transfer system in which the relative contributions of Sendai virus–specific effector– and central–memory cells to recall responses in the lung could be directly compared on a per-cell basis. These studies demonstrated that the relative contribution of effector– and central–memory cells to the recall response in the lung varied depending on how recently memory had been established (28, 29). Although effector–memory CD8$^+$ T cells dominated the recall response relatively soon after infection (up to 6 mo after infection), central–memory CD8$^+$ T cells dominated the recall response at later times (12 mo after infection). Furthermore, the data showed that on a per-cell basis, both central– and effector–memory T cells isolated from the spleens of mice 1 yr after infection mediated dramatically stronger recall responses to Sendai virus infection than the same subpopulations of memory T cells isolated 1 mo after infection (28). The overall conclusion from these and other studies is that there is no direct or generalized relationship between central– and effector–memory phenotype of the memory T cell pool and the ultimate composition of the recall response at the site of infection.

Here, we define three distinct subpopulations of memory CD8$^+$ T cells that are superior to central– and effector–memory phenotype in predicting recall efficacy. The data resolve discrepancies regarding the contribution of central– and effector–memory T cells to recall responses and suggest an alternative or additional scheme to classify memory T cells. The findings extend our understanding of how recall responses are generated and indicate which types of memory T cells should be targeted by vaccines.

RESULTS

Activation markers identify distinct memory CD8$^+$ T cell subsets

Studies addressing the contribution of central– and effector–memory CD8$^+$ T cell subpopulations to the recall response have been contradictory and inconclusive (16, 21–24, 26, 28).

Therefore, we speculated that recall efficacy correlated with other characteristics of memory cells that were independent of their central– or effector–memory status. To test this notion, we analyzed the phenotype of memory $CD8^+$ T cells generated by intranasal Sendai virus infection (specific for the immunodominant $NP_{324–332}/K^b$ epitope) with a particular emphasis on the expression of markers that distinguish quiescent and semi-activated memory T cell subsets, such as CD27, CD43 (activated isoform), and CD127 (30–33). As shown in Fig. 1, analyses of CD27 and CD43 (1B11) expression at 1 mo after Sendai virus infection divided $NP_{324–332}/K^b$-specific T cells into three distinct subpopulations: $CD27^{hi}/CD43^{hi}$, $CD27^{hi}/CD43^{lo}$, and $CD27^{lo}/CD43^{lo}$. Further analysis revealed that the chemokine receptor CXCR3 was coordinately expressed with CD27 (not depicted) and that the same three subpopulations of memory $CD8^+$ T cells could also be defined by CXCR3/CD43 expression (Fig. 1 A). There was also a similar pattern of expression for CD127 in that all of the $CD127^+$ cells were also $CD27^+$. The correlation between CD127 and CD27 is illustrated in Fig. 1 B. Analysis of the three coordinated memory T cell subsets at various times after infection revealed that the $CD27^{hi}/CD43^{lo}$ subpopulation progressively dominated the memory T cell pool, representing ~90% of the antigen-specific T cells detected at 2 yr after infection (Fig. 1 A). In contrast, the $CD27^{lo}/CD43^{lo}$ subpopulation progressively declines and disappeared by about 1 yr after infection. Thus, the representation of these distinct subpopulations within the total memory $CD8^+$ T cell pool progressively changes over time.

The identification of three distinct memory populations expressing coordinated patterns of markers was of interest because very few markers are coordinately expressed on memory T cells. One question was whether these subpopulations corresponded to the central– ($CD62L^{hi}$) and effector– ($CD62L^{lo}$) memory $CD8^+$ T cells subsets. Consistent with previous reports (3, 28), ~10% of Sendai virus $NP_{324–332}/K^b$-specific memory $CD8^+$ T cells expressed a central–memory ($CD62L^{hi}$) phenotype at 1 mo after infection, and this percentage rose to 90% at 12 mo after infection. Regardless of the time point, both central– and effector–memory $CD8^+$ T cells were present in roughly equal frequencies in each of the subpopulations ($CXCR3^{hi}/CD43^{hi}$, $CXCR3^{hi}/CD43^{lo}$, and $CXCR3^{lo}/CD43^{lo}$; Fig. 1 C). Collectively, the data indicate that the division of memory $CD8^+$ T cells into three major subpopulations is independent of central– or effector–memory status.

To determine whether these subpopulations of memory T cells expressed markers typically associated with T cell senescence or exhaustion, we analyzed the expression of killer cell lectin-like receptor G1 (KLRG1), a marker of senescent cells linked to poor in vitro proliferative capacity, and programmed death-1 (PD-1), a marker of T cell exhaustion (34–36). As shown in Fig. 1 D, ~40% of the $CD27^{lo}/CD43^{lo}$ cells expressed KLRG1, whereas none of the cells expressed PD-1. The data suggest that the $CD27^{lo}/CD43^{lo}$ population may include cells that have the characteristics of immune senescence.

The three memory cell subpopulations ($CD27^{hi}/CD43^{hi}$, $CD27^{hi}/CD43^{lo}$, and $CD27^{lo}/CD43^{lo}$) were not a unique feature of Sendai virus or a mucosal route of infection. As shown in Fig. 1 E, identical subpopulations were also identified in the pool of memory $CD8^+$ T cells elicited by intranasal influenza virus infection (specific for both the influenza $NP_{366–374}/D^b$ and $PA_{224–233}/D^b$ epitopes). The same subpopulations of memory $CD8^+$ T cells were also observed after intraperitoneal (systemic) Sendai and influenza virus infection (not depicted).

We next asked whether the rate of homeostatic turnover differed for each of the three memory cell subpopulations ($CD27^{hi}/CD43^{hi}$, $CD27^{hi}/CD43^{lo}$, and $CD27^{lo}/CD43^{lo}$; references 37 and 38). Mice were intranasally infected with Sendai virus and 1 mo later were administered BrdU for 14 d in the drinking water. Memory T cells in each of the sub populations became $BrdU^+$ over this timeframe, indicating that all subpopulations were being maintained to some extent by homeostatic proliferation (Fig. 2). However, the rate of BrdU accumulation was markedly different for each of the

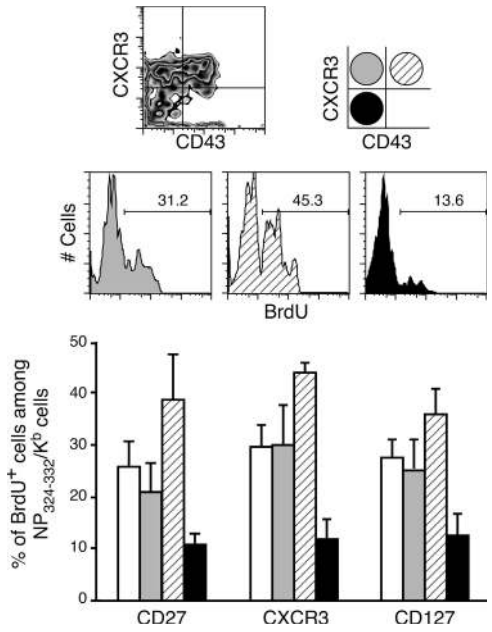

Figure 2. Memory $CD8^+$ T cell subpopulations homeostatically proliferate at different rates. Mice (1 mo after Sendai virus infection) were administered BrdU in the drinking water for 14 d. Splenocytes were then stained with Sendai $NP_{324–332}/K^b$ tetramer and monoclonal antibodies. The cells were gated first on $tetramer^+/CD8^+$ cells and then subgated into $CXCR3^{hi}/CD43^{lo}$, $CXCR3^{hi}/CD43^{hi}$, and $CXCR3^{lo}/CD43^{lo}$ subpopulations (as indicated by the flow cytometric plot and schematic diagram, top panels). The frequency of $BrdU^+$ cells was then determined in each subpopulation. The bar chart shows the percentage of $BrdU^+$ cells in total $tetramer^+/CD8^+$ cells (pen bars) or in $tetramer^+/CD8^+$ cells gated on each of the memory T cell subpopulations based on either CD27×CD43 expression, CXCR3×CD43 expression, or CD127×CD43 expression (shaded bars use the same schematic indicated in the top right of the figure). The values are means ± SD of three individual mice and are representative of three independent experiments.

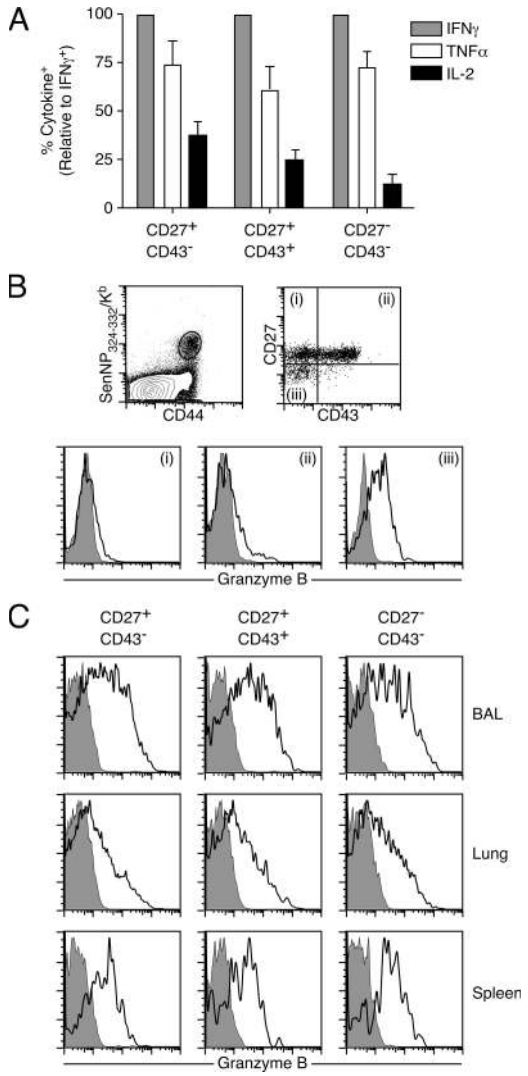

Figure 3. Memory CD8$^+$ T cell subpopulations display similar effector functions after antigen challenge. (A) Splenic memory CD8$^+$ T cells from C57BL/6 mice were isolated 1 mo after infection and flow cytometrically sorted into subpopulations based on activation marker expression (CD27^{hi}/CD43^{lo}, CD27^{hi}/CD43^{hi}, and CD27^{lo}/CD43^{lo}). Aliquots of the sorted cells were stained with Sendai NP$_{324–332}$/K^b tetramer to determine the frequency of antigen-specific cells within each subset. Sorted populations were co-cultured with CD45.1$^+$ splenocytes pulsed with 1 μg Sendai NP$_{324–332}$ peptide for 5 h in the presence of brefeldin A, and IFN-γ, TNF-α, and IL-2 were measured by intracellular staining and flow cytometry. The data are plotted as the frequency of cytokine$^+$ cells and normalized to IFN-γ expression. The data are derived from three independent experiments for each subpopulation. (B) Splenocytes from resting Sendai memory mice were divided into memory CD8$^+$ subpopulations by staining with Sendai NP$_{324–332}$/K^b tetramer, CD27, and CD43 (top), and granzyme B expression was measured in each subpopulation as denoted by roman numerals (bottom). In each of the bottom panels, granzyme B expression is denoted by the open histogram, and isotype control staining is shown by the shaded histogram. The data are representative of two independent experiments. (C) Splenic memory CD8$^+$ T cell subsets were isolated from C57BL/6 by cell sorting as described above, and the number of Sendai-specific cells within each subpopulation was determined by staining with Sendai NP$_{324–332}$/K^b tetramer. 3,000–5,000 Sendai-specific cells from each subpopulation were transferred intravenously into individual naive CD90.1$^+$ recipient mice, and the recipient mice were infected with 250 EID$_{50}$ Sendai virus 24 h later. Bronchoalveolar lavage, lung parenchyma, and spleen were harvested 11 d after infection, and granzyme B expression was measured in Sendai-specific donor cells. The histograms shown are gated on Sendai NP$_{324–332}$/K^{b+} CD90.2$^+$ donor cells, with granzyme B expression denoted by the open histogram and isotype control staining denoted by the shaded histogram. The phenotype of the sorted memory donor subpopulations transferred is listed at the top of each column. The data are representative of two independent experiments, with three recipient mice for each memory subset.

three subpopulations. For example, the CXCR3^{lo}/CD43^{lo} subpopulation accumulated BrdU at one quarter the rate of the CXCR3^{hi}/CD43^{hi} subpopulation. The slower turnover rate of the CXCR3^{lo}/CD43^{lo} subpopulation may account for the progressive disappearance of this population from the memory T cell pool over time. The same patterns of homeostatic proliferation were observed when the three subpopulations were identified on the basis of CD27 (consistent with the coordinate expression of this marker with CXCR3) and CD127 (Fig. 2).

We also analyzed the effector functions of the different memory T cell subpopulations. All of the tetramer$^+$ cells in each subpopulation were functional in terms of the capacity to secrete IFN-γ in an intracellular cytokine assay, consistent with previous studies showing that the entire NP$_{324–332}$/K^b-specific CD8$^+$ memory T cell population is functional in terms of IFN-γ secretion (reference 3 and not depicted). In addition, the fraction of IFN-γ$^+$ cells that produced TNF-α and IL-2 was similar for each subpopulation, although the frequency of IL-2$^+$ cells was highest among the CD27^{hi}/CD43^{lo} subpopulation (Fig. 3 A). In contrast, there was a notable difference in granzyme B expression among the three memory T cell subpopulations. Although the CD27^{hi}/CD43^{hi} and CD27^{hi}/CD43^{lo} cells were granzyme B$^-$, the CD27^{lo}/CD43^{lo} cells were granzyme B$^+$ (Fig. 3 B). However, granzyme B was expressed by all three subpopulations in the context of a recall response to Sendai virus infection (Fig. 3 C).

Memory CD8$^+$ T cell subpopulations differ in recall efficacy in the lung

CD8$^+$ T cell recall responses to secondary respiratory virus infections are characterized by an increased accumulation of activated effector CD8$^+$ T cells within the lungs and lung airways. To determine the individual contributions of the different memory T cell subpopulations to the accumulation of these cells in the lungs, we used a dual adoptive transfer approach in which we could directly compare the responses of two separate populations of memory T cells in the same animal under the same infection conditions (28, 29). Initial experiments were focused on memory T cells that were either positive or negative for CD43 expression. Spleen cells from C57BL/6 and B6-CD45.1 donors were enriched for CD8$^+$ cells on a negative selection column and

flow cytometrically sorted on the basis of CD44 and CD43 expression. The $CD44^{hi}/CD43^{hi}$ and $CD44^{hi}/CD43^{lo}$ subpopulation from each donor was then mixed together, such that the ratio of $NP_{324–332}/K^b$ cells was 1:1, and intravenously injected into B6-CD90.1 recipient mice. 1 d later, recipient mice were intranasally infected with Sendai virus, and $NP_{324–332}/K^b$-specific T cells were analyzed 11 d later in the lung airways (bronchoalveolar lavage), lung parenchyma, pleural cavity lavage, mediastinal lymph nodes (MLNs), and spleens. Cells derived from each donor and from the host were distinguished on the basis of CD90 and CD45 expression, and the ratio of the response of the two donors was determined (39). An example of the sorting/transfer strategy and the data generated is presented in Fig. 4. The strength of this basic approach is that the response of two polyclonal (i.e., nontransgenic) populations of cells is compared in the same animal under identical infection conditions. In addition, it effectively integrates all of the factors involved in the accumulation of activated effector T cells at the site of infection, such as their capacity to migrate to lymph nodes before infection, the overall proliferative and death rates of the responding cells, and the capacity of the cells to migrate to inflammatory sites (27). As shown in Fig. 5, data obtained from several experiments established that $CD43^{lo}$ memory $CD8^+$ T cells were two- to fivefold more efficient than $CD43^{hi}$ cells at mediating the recall response to Sendai virus infection in the airways, parenchyma, and pleural cavities of the lung (similar data were obtained in the MLN and spleen; not depicted). This relative dominance of the $CD43^{lo}$ subpopulation was observed regardless of whether the memory T cells were isolated 1 or 6 mo after the primary infection (Fig. 5). These data support the finding that $CD43^{lo}$ memory $CD8^+$ T cells mediate stronger recall responses than $CD43^{hi}$ cells in terms of their accumulation at the site of infection, and this dominance is maintained over the long term.

Using the same approach, we then compared the recall efficacy of $CD27^{hi}$ and $CD27^{lo}$, as well as $CXCR3^{hi}$ and $CXCR3^{lo}$, memory subpopulations. As shown in Fig. 5, data from several independent experiments showed that the $CD27^{hi}$ and $CXCR3^{hi}$ memory subpopulations were 2–10-fold more efficient than their counterparts at contributing to the recall responses in different compartments of the lung. In the case of CXCR3 sorted cells, we also analyzed the phenotype of effector $CD8^+$ T cells that accumulated in the lungs of host mice on day 10 of infection. Donor memory cells retained their original CXCR3 phenotype in both the lung and spleen (not depicted), suggesting that expression of this chemokine receptor is not necessary for memory cell activation or migration into a site of inflammation. The original phenotypic

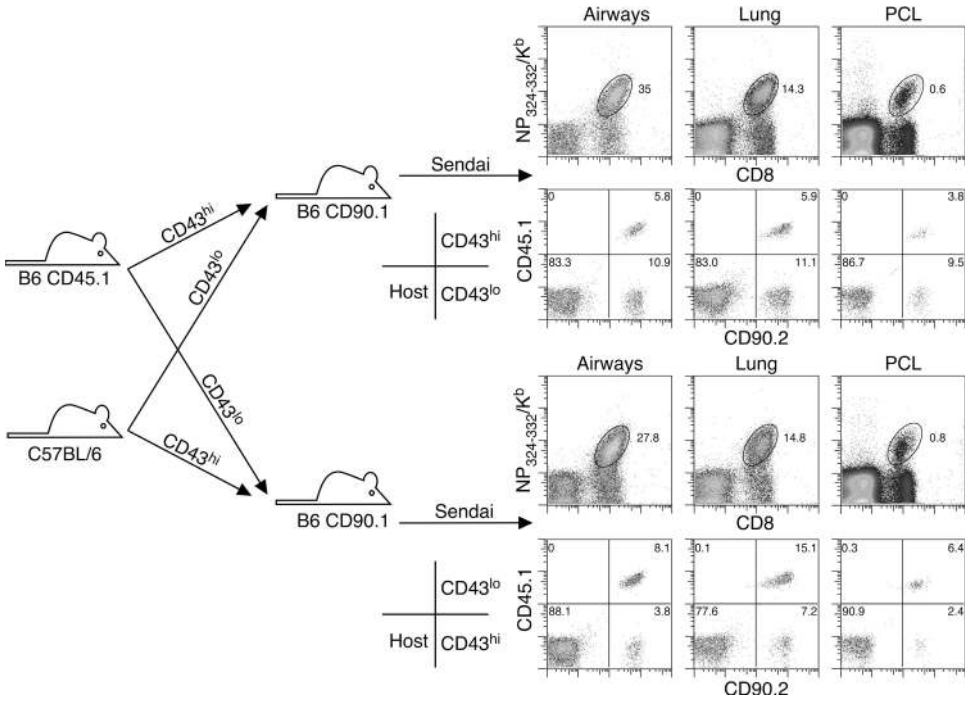

Figure 4. Recall efficacy of $CD43^{hi}$ and $CD43^{lo}$ memory T cells. Donor mice (CD45.2/CD90.2 and CD45.1/CD90.2) were infected with Sendai virus and splenocytes isolated 1 mo later. Cells were enriched for $CD8^+$ cells on negative selection columns and then sorted into $CD44^{hi}/CD43^{hi}$ and $CD44^{hi}/CD43^{lo}$ subpopulations by FACS. Sorted subsets were combined from each donor, such that the number of Sendai $NP_{324–332}/K^{b+}$ cells derived from each donor was equivalent (usually 10,000 $tetramer^+$ cells comprised of 5,000 cells from each donor) and intravenously transferred into recipient mice (CD45.2/CD90.1). 1 d after transfer, the recipient mice were then intranasally challenged with Sendai virus, and the indicated tissues were analyzed 11 d later. The flow cytometric profiles in the bottom rows of each panel are gated on $tetramer^+/CD8^+$ cells (indicated in the oval gate in the top panels). The data are representative from two recipient mice.

pattern was also retained through day 35 after transfer (day 34 after infection), when the donor cells had returned to a resting memory phenotype (Fig. 6, A and B). Furthermore, the CXCR3^{lo} cells retained their original CD127^{lo} and CD43^{lo} phenotype when analyzed at this time point. However, retention of the original phenotype by effector– or secondary memory CD8$^+$ T cells was not characteristic of cells sorted on the basis of CD43 expression inasmuch as each of the CXCR3^{hi}/CD43^{hi} and CXCR3^{hi}/CD43^{lo} subpopulations was capable of generating all three of the memory T cell subpopulations after reactivation (not depicted). Collectively, the data suggest that memory CD8$^+$ T cells expressing either a CD27^{hi}, CXCR3^{hi}, or a CD43^{lo} phenotype mediate the strongest recall response. Furthermore, cells expressing either a CXCR3^{hi} or CXCR3^{lo} phenotype retain this phenotype throughout the response and into the establishment of secondary memory cells. However, it is currently unclear whether this phenotype is retained over the long term.

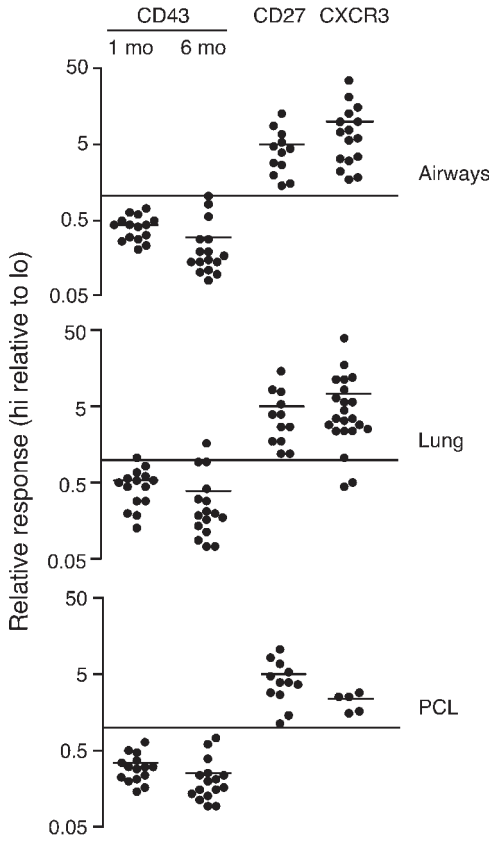

Figure 5. Memory CD8$^+$ T cell subpopulations differ in their capacity to mediate recall responses. Splenic CD8$^+$ T cells were isolated at 1 mo after infection (and additionally at 6 mo after infection for CD43 only) and flow cytometrically sorted into CD43$^{hi/lo}$, CD27$^{hi/lo}$, or CXCR3$^{hi/lo}$ subpopulations. The cells were then tested for their capacity to contribute to a recall response to intranasal Sendai virus challenge using the strategy outlined in Fig. 4. The relative response in each tissue was calculated as the percentage of Sendai NP$_{324–332}$/K^b-specific T cells derived from one donor population divided by the percentage from the second donor population (i.e., the ratio of donor cell populations recruited to the tissue). Each symbol represents data from an individual recipient mouse. Data are from four independent experiments for CD43 (1 and 6 mo after infection) and CD27 and six independent experiments for CXCR3. Pleural cavity lavages were not collected in all of the CXCR3 experiments.

CD27^{hi}/CD43^{lo} memory CD8$^+$ T cells mediate the strongest recall response in the lung

The data thus far indicate that memory CD8$^+$ T cells with either a CD27^{hi} or a CD43^{lo} phenotype mounted superior recall responses. Collectively, these data suggest that the CD27^{hi}/CD43^{lo} memory CD8$^+$ T cell subpopulation mounted the strongest recall response in the lung. To test this idea, we sorted memory CD8$^+$ T cells from the spleens of mice that had recovered from a prior Sendai virus infection (1 mo after infection) into the three memory T cells subpopulations and used dual adoptive transfer studies to compare the ability of each subpopulation to mount a recall response (the sorting strategy is illustrated in Fig. S1, available at http://www.jem.org/cgi/content/full/jem.20070322/DC1). Because CXCR3 and CD27 are coordinately expressed (Fig. 1 and not depicted), the anti-CXCR3 antibody, rather than the anti-CD27 antibody, was used for sorting as it yielded superior separation of the memory cell subsets. These three-way sort/dual

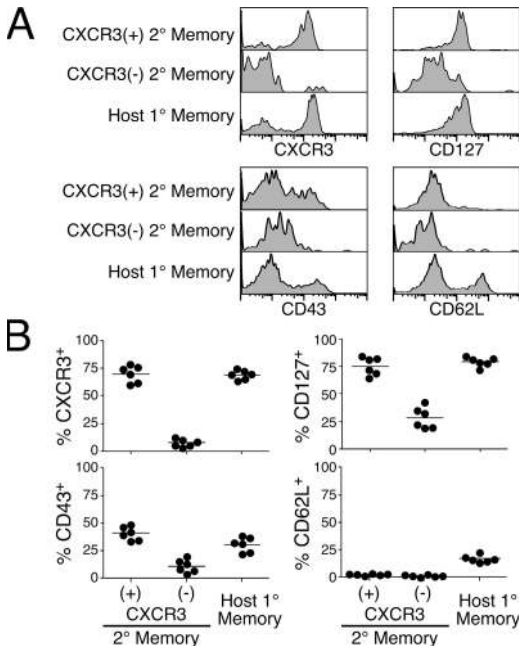

Figure 6. Activation marker phenotype is retained on secondary memory CD8$^+$ T cells. Mice from the dual adoptive transfer of CXCR3$^+$ and CXCR3$^-$ memory CD44$^+$/CD8$^+$ T cells in Fig. 5 were analyzed on day 34 after infection. Spleens were harvested, and the expression of CXCR3, CD127, CD43, and CD62L was analyzed on tetramer$^+$/CD8$^+$ gated cells from the host (1° memory) and each of the transferred populations (CXCR3$^+$ 2° memory and CXCR3$^-$ 2° memory). Representative staining from one mouse is shown in A. (B) Cumulative data from independent transfer experiments. Each symbol represents an individual mouse. The data are representative of three independent experiments.

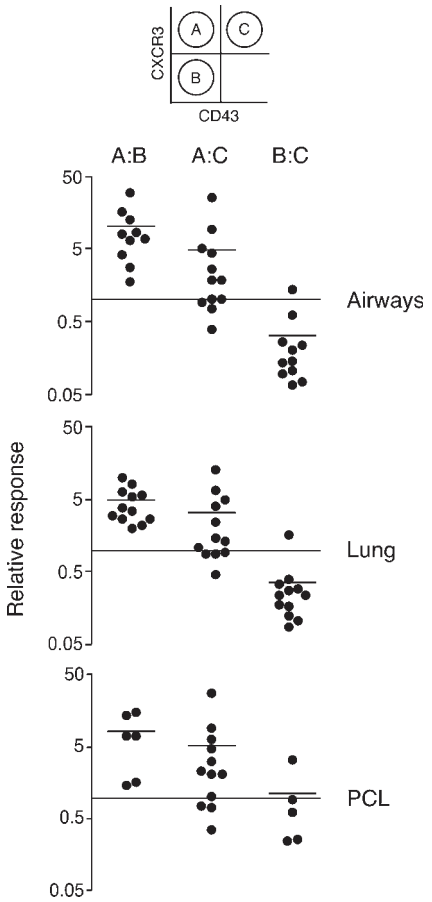

Figure 7. CD43^{lo}/CXCR3^{hi} memory CD8$^+$ T cell subset mediates the strongest recall responses. Donor mice (CD45.2/CD90.2 and CD45.1/CD90.2) were infected with Sendai virus. 1 mo later, splenocytes were enriched for CD8$^+$ cells using negative selection columns and flow cytometrically sorted into CD44^{hi}/CD43^{lo}/CXCR3^{hi} (subpopulation A), CD44^{hi}/CD43^{lo}/CXCR3^{lo} (subpopulation B), and CD44^{hi}/CD43^{hi}/CXCR3^{hi} (subpopulation C) as illustrated in the schematic and using the strategy outlined in Fig. S1. Cells were then tested pair wise in dual adoptive transfer experiments for their capacity to contribute to a recall responses to intranasal Sendai virus challenge, as described in the legends to Figs. 4 and 5. Each symbol represents data from an individual recipient mouse, and the data are derived from four independent experiments.

adoptive transfer experiments clearly demonstrate that the three CXCR3^{hi}/CD43^{hi}, CXCR3^{hi}/CD43^{lo}, and CXCR3^{lo}/CD43^{lo} memory cell subpopulations differ in their capacity to mount recall responses in the lungs after secondary Sendai virus challenge (Fig. 7). CXCR3^{hi}/CD43^{lo} cells (labeled as population A in Fig. 7) were superior to both CXCR3^{lo}/CD43^{lo} cells (labeled as population B) and CXCR3^{hi}/CD43^{hi} cells (labeled as population C). Furthermore, CXCR3^{lo}/CD43^{lo} cells (population B) mounted the weakest recall response compared with the other two memory T cell populations. These data, together with the fact that CXCR3 and CD27 are coordinately expressed, support a hierarchy of CD27^{hi}/CD43^{lo} > CD27^{hi}/CD43^{hi} > CD27^{lo}/CD43^{lo} memory cells in terms of mediating recall responses in the lung.

Vaccination elicits different subpopulations of memory CD8$^+$ T cells

The differences in recall efficacy of memory CD8$^+$ T cell subpopulations have substantial implications for the design of vaccines. Therefore, we compared the capacity of Sendai $NP_{324–332}$ peptide-loaded dendritic cells or peptide administered in CFA to elicit memory CD8$^+$ T cells. In the course of these analyses, we observed that Sendai $NP_{324–332}$ peptide/CFA induced very high frequencies of CD27^{lo}/CD43^{lo} memory CD8$^+$ T cells, predicted by our previous analysis to be poor responders to secondary Sendai virus challenge (Fig. 8 A). Although the ratio of the three CD27^{hi}/CD43^{lo}, CD27^{hi}/CD43^{hi}, and CD27^{lo}/CD43^{lo} memory CD8$^+$ T cell subpopulations was ~1:1:1 in mice that had recovered from a prior Sendai virus infection (1 mo after infection), the ratio of these subpopulations was ~1:2:6 in peptide/CFA-vaccinated mice. Also, a substantial population of cells with a fourth phenotype (CD27^{lo}/CD43^{hi}) was observed in peptide CFA-vaccinated mice. In addition, the memory T cell pool elicited by peptide CFA vaccination was exclusively of the effector–memory phenotype, and ~90% of the cells were CD127^{hi} (Fig. 8 B). Consistent with data generated from mice that had recovered from a Sendai virus infection, KLRG1$^+$ cells were highly enriched among the CD27^{lo} subpopulations of memory T cells elicited by peptide CFA vaccination (Fig. 8 C). Because CD27^{lo} cells represented a greater proportion of the memory pool generated by CFA vaccination (compared with viral infection), a much higher frequency of the total $NP_{324–332}/K^b$-specific population was also KLRG1$^+$ (Fig. 8 D).

Based on these findings, we hypothesized that the overall pool of $NP_{324–332}/K^b$-specific memory T cells generated by $NP_{324–332}$ peptide/CFA vaccination would mount weaker recall responses compared with the pool of $NP_{324–332}/K^b$-specific memory T cells generated by a prior Sendai virus infection. Because peptide/CFA vaccination induced sufficient numbers of memory T cells available for dual transfer studies, we were able to test this hypothesis by directly comparing the recall efficacy of memory T cells isolated from vaccinated mice to those isolated from mice that had recovered from a prior Sendai virus infection. As shown in Fig. 9 A, data from several experiments demonstrated that memory CD8$^+$ T cells from peptide/CFA-vaccinated mice were 10-fold less efficient than memory cells from Sendai virus–infected mice at contributing to a recall response to Sendai virus infection in the lung airways and parenchyma (similar data were obtained in the MLN and spleen; not depicted). Thus, consistent with our phenotypic analyses and our hypothesis, peptide/CFA vaccination generated comparatively poor quality memory T cells.

To investigate the memory CD8$^+$ T cells generated by peptide/CFA vaccination further, we isolated memory subpopulations on the basis of CD43^{hi}/CD43^{lo} or CXCR3^{hi}/CXCR3^{lo} expression and compared their abilities to contribute to the recall response to intranasal Sendai virus infection. Consistent with memory cells generated by Sendai virus infection, CXCR3^{hi} cells were superior to CXCR3^{lo} cells in mounting

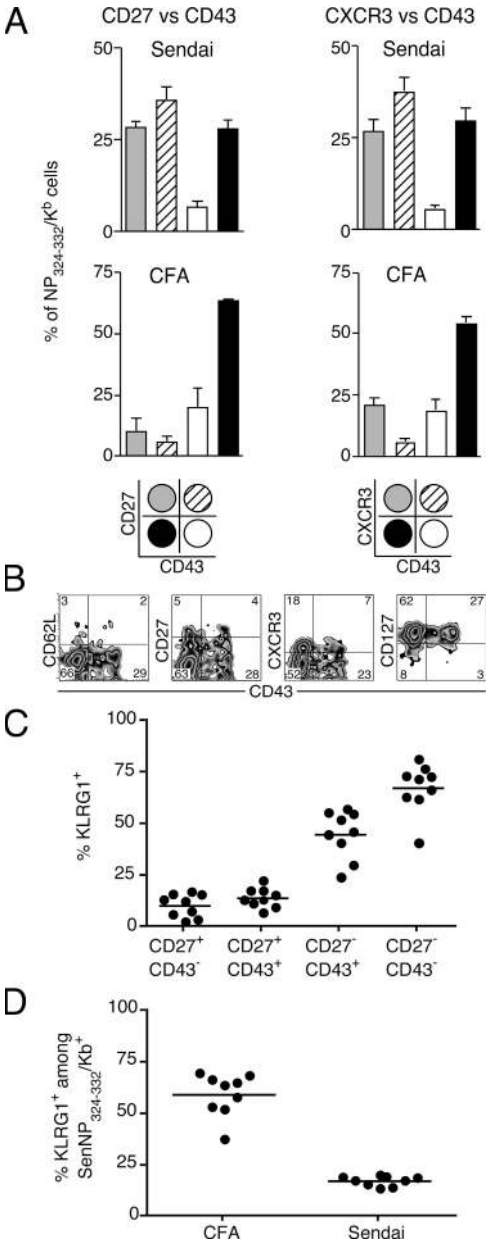

Figure 8. Memory CD8$^+$ T cells generated by peptide/CFA vaccination are enriched for cells with a poorly proliferative phenotype. Mice were either intranasally infected with Sendai virus or subcutaneously vaccinated with Sendai $NP_{324–332}$ peptide/CFA and analyzed 1 mo later. (A) Phenotype of tetramer$^+$/CD8$^+$ cells based on the expression of CD27 and CD43 (left) or CXCR3 and CD43 (right) in Sendai virus–immune mice (top panels) or peptide/CFA-vaccinated mice (bottom panels). Each subpopulation is indicated by the shading pattern in the schematic under the bar charts. The data show the means ± SD of three individual mice. (B) Coexpression of CD43, CD62L, CD27, CXCR3, and CD127 on tetramer$^+$/CD8$^+$ gated cells from $NP_{324–332}$/CFA-vaccinated mice 1 mo after vaccination. Numbers represent the percentage of cells in each quadrant. The data are representative of three individual mice. (C) Splenocytes from peptide/CFA-vaccinated mice were gated on tetramer$^+$/CD8$^+$ cells and divided into subsets based on the expression of CD27 and CD43. The frequency of KLRG1$^+$ cells within each subset is plotted for individual mice. (D) The frequency of KLRG1$^+$ cells among total Sendai $NP_{324–332}$/K^b+ cells after peptide/CFA vaccination or Sendai virus infection are plotted for individual mice. The data for C and D are combined from two independent experiments.

recall responses (Fig. 9 B). Interestingly, CD43^{hi} cells resulting from peptide/CFA-vaccinated mice were superior to CD43^{lo} cells, a finding opposite to that seen with memory cells generated by Sendai virus infection. However, this difference is fully consistent with the fact that CD43^{lo} cells isolated from peptide/CFA-vaccinated mice are dominated by poorly responsive CXCR3^{lo}/CD43^{lo} cells (Fig. 8 A). In summary, the distribution of distinct memory CD8$^+$ T cell subpopulations generated by vaccination or infection can accurately forecast the recall potential of the memory T cell pool.

DISCUSSION

Despite progress over the last few years in characterizing the properties of memory T cells, it is still not understood how different types of memory T cells actually contribute to recall responses or which memory T cells are the most appropriate for different pathogens. A key advance has been the realization that memory cells express distinct patterns of homing receptors. This in turn has led to the idea that effector–memory T cells in the periphery play a key role in mediating immediate responses to mucosal or peripheral infections, whereas central–memory T cells are more important for mediating proliferative responses to systemic infections. However, this idea has been difficult to reconcile with data showing that both central– and effector–memory T cells mount potent proliferative responses (16, 21–26, 28). In this study, we have analyzed T cell memory subpopulations from the perspective of activation markers. The data indicate that patterns of CD27 and CD43 (1B11) expression define three distinct subpopulations of memory CD8$^+$ T cells that differ significantly in their capacities to contribute to the accumulation of effector cells in the lungs during a respiratory virus challenge. These subpopulations coordinately express an array of other markers associated with activation status, including CXCR3, CD127, and KLRG1, and are independent of effector– and central–memory status (23, 31, 34, 40). In general, there appears to be an inverse correlation between activation status and proliferative potential, such that cells with the most "rested" phenotype have the capacity to mediate the strongest recall responses. For example, the subpopulation of memory T cells able to mediate the strongest recall response was shown to express a CD27^{hi}/CD43^{lo} phenotype (41). In contrast, the subpopulation of memory T cells that mediated the weakest recall responses expressed a CD27^{lo}/CD43^{lo} phenotype. Indeed many, but not all, of the cells in this latter subpopulation expressed characteristics of senescent T cells, including expression of KLRG1. Although all of the subpopulations of memory cells are based on markers typically associated with activation, the cells are nevertheless small, nonblasted, and do not express acute activation markers such as CD69 or CD25. Thus, our data support a new functional

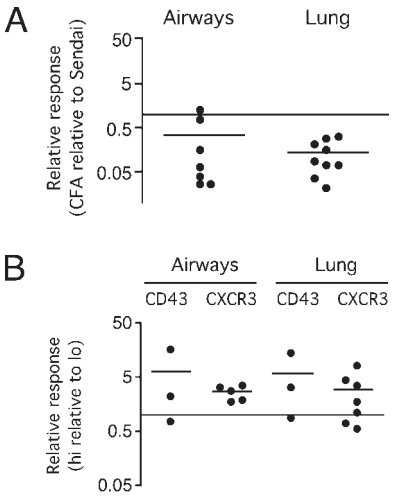

Figure 9. Memory CD8+ T cells generated by peptide/CFA vaccination exhibit poor recall efficacy. (A) Recall efficacy of memory CD8+ T cells generated by Sendai virus infection and peptide/CFA vaccination. C57BL/6 donor mice were subcutaneously vaccinated with Sendai virus nucleoprotein peptide ($NP_{324–332}$) emulsified in CFA, and CD90.1 donor mice were intranasally infected with Sendai virus. 1 mo later, splenic $CD8^+/CD44^{hi}$ memory cells were isolated and analyzed in dual adoptive transfer experiments for their capacity to contribute to recall responses to intranasal Sendai virus challenge, as described in the legend to Figs. 4 and 5. Each symbol represents data from an individual recipient mouse, and the data are derived from three independent experiments. (B) Comparison of the relative responses of memory CD8+ T cell subpopulations elicited by peptide/CFA vaccination. Mice were vaccinated or infected as described for A, and CD8+ enriched cells were sorted into $CD44^{hi}/CD43^{hi}$ and $CD44^{hi}/CD43^{lo}$ (or $CD44^{hi}/CXCR3^{hi}$ and $CD44^{hi}/CXCR3^{lo}$) by FACS. The sorted subsets were then compared by dual adoptive transfer as described for A. Each symbol represents data from an individual recipient mouse, and two independent experiments were performed for CD43 and CXCR3.

classification of memory CD8+ T cells that is based on activation phenotype rather than the widely accepted central– and effector–memory T cell classification (based on markers such as CD62L and CCR7). The most potent memory T cells, in terms of their proliferative capacity, express the most quiescent activation phenotype, and these cells tend to accumulate over time. This population also becomes increasingly dominated by cells with a central–memory phenotype ($CD62L^{hi}$) and ultimately comes to most resemble naive T cells. Overall, these findings suggest a pattern of memory T cell differentiation in which many markers and properties change over time, but at different rates.

The division of memory cells into subpopulations based on the expression of activation markers may help explain certain features of CD8+ T cell memory. First, we have previously shown that the recall efficacy of memory CD8+ T cells progressively improves over time (28). This observation could not be explained by changes in the distribution of effector– and central–memory T cells over time, as the improvement occurred on a per-cell basis and within both of these subpopulations. However, the data here show that there is a progressive loss of memory cell subpopulations that express a weak ($CD27^{lo}/CD43^{lo}$) or intermediate ($CD27^{hi}/CD43^{hi}$) proliferative capacity from the total memory T cell pool. Although these less responsive phenotypes of cells represented ~70% of the total memory T cell pool at 1 mo after infection, they only represented 5–10% of the population at 2 yr after infection (with the very poorly responding $CD27^{lo}/CD43^{lo}$ subpopulation essentially gone by about 1 yr after infection). Thus, a progressive loss of poorly responding memory T cells may explain the finding that that efficacy of the total memory T cell pool increases over time. Second, we have previously shown that the relative contributions of effector– and central–memory T cell subpopulations to recall responses differ dramatically between recently generated and long-term pools of memory T cells (28, 29). Changes in the distribution of memory cells expressing activation markers within these subpopulations over time potentially explain these differences. For example, the strongly responsive $CD27^{hi}/CD43^{lo}$ cells become increasingly represented in central–memory cells over time (for example, compare the distribution of $CD43^{hi}$ and $CD43^{lo}$ cells in the central– and effector–memory T cell pools at 1 and 12 mo after infection in Fig. 1). Third, our unpublished studies had suggested that although peptide/CFA vaccination was effective at establishing large numbers of memory T cells, it was relatively poor at eliciting recall responses. Our current observation that peptide/CFA vaccination generated very high frequencies of poorly responsive $CD27^{lo}/CD43^{lo}$ memory CD8+ T cells likely explains the overall weak recall response elicited by this vaccine strategy. Thus, enumeration of these newly described memory CD8+ T cell subpopulations allows one to predict the overall efficacy of a recall response.

The significance of the CD27 and CD43 activation markers on memory T cells is poorly understood. CD27 is a TNF receptor family member that functions as a T and B cell costimulatory molecule (32, 42, 43). This marker has previously been shown to correlate with effector functions in humans (44). CD43 occurs as two distinct glycoforms (115 and 130 kD) of which the 130 kD glycoform is associated with T cell activation and is specifically detected by the 1B11 antibody (45). It is involved in cell adhesion and may also regulate apoptosis during acute and memory phases of an immune response (33, 46–48). Although these markers clearly regulate different aspects of the immune response, it is unlikely that they actually mediate the differences in recall response observed in the current studies. Rather, they are probably surrogate markers of intrinsic programmed states of the memory T cell that affects recall efficacy. One possibility is that this phenotype is associated with optimal access to sites of antigen presentation within lymphoid tissues, although this is not entirely consistent with patterns of CD62L expression (27). Another possibility is that these cells may have undergone less expansion during the acute response and therefore retain more proliferative potential (49). We are currently investigating these possibilities.

The lack of any relationships between activation marker status and central/effector–memory phenotypes suggests that

these two characteristics of memory T cells are completely independent of each other. Several studies have addressed the relative recall efficacy of central– and effector–memory T cells, and results from these studies have been either contradictory or inconclusive, probably reflecting the use of different infection models (16, 21–28). Also, these studies did not account for the presence of KLRG1-expressing senescent cells within the populations of memory T cells examined (as discussed above; reference 34). Other issues to be considered are the migration and resulting distribution of the cells in adoptive transfer experiments. Cells separated on the basis of CD62L tend to distribute differently in recipients after adoptive transfer with $CD62L^{hi}$ cells tending to localize preferentially in the lymph nodes (28, 29). An ability to localize the lymph nodes is likely important for responses that depend on dendritic cell and antigen trafficking to the lymph nodes (27). In these current studies, we found no evidence that memory $CD8^+$ T cells expressing different activation markers had different patterns of migration to the lymph nodes (unpublished data). These data further suggest that activation markers (CD27/CD43) and migration markers (CD62L/CCR7) define distinct, and unrelated, characteristics of memory cells. Thus, activation marker expression may influence the general capacity of memory T cells to mediate a recall response, whereas migration markers may dictate the capacity of memory T cells to migrate to sites of antigen deposition.

In summary, the data presented here suggest that the expression of certain activation markers on memory $CD8^+$ T cells is a better predictor of recall efficacy than central– and effector–memory phenotype. Separation of memory cell subpopulations by these phenotypes helps resolve prior discrepancies regarding the contribution of central– and effector–memory T cells to recall responses, and also supports the use of these phenotypes as an alternative or additional scheme to classify memory T cells. Although central– and effector–memory phenotypes are markers of memory T cell–trafficking patterns, activation marker expression likely indicates different functional qualities of memory T cells. Clearly, both factors need to be taken into consideration during vaccine development.

MATERIALS AND METHODS

Virus, mice, infection, and vaccination. Sendai virus (Enders strain) and influenza virus A/HK-x31 were grown, stored, and titered as described previously (50). 8–12-wk-old female C57BL/6J, B6.SJL-*Ptprc*a Pep3/BoyJ (CD45.1), and B6.Pl-*Thy1*a/Cy (CD90.1) mice (The Jackson Laboratory) were anesthetized and intranasally infected with 250 50% egg infectious doses (EID_{50}) of Sendai virus or 600 EID_{50} of x31 influenza virus. Vaccination was performed with 50 μg of Sendai virus nucleoprotein peptide ($NP_{324–332}$) emulsified in 100 μl CFA by subcutaneous injection in the base of the tail. All animal studies were approved by the Trudeau Institute Animal Care and Use Committee.

Flow cytometric analyses. Splenocytes were panned on goat anti–mouse IgG H+L (Jackson ImmunoResearch Laboratories) -coated flasks and stained with APC-conjugated tetramers (Sendai $NP_{324–332}/K^b$, Flu $NP_{366–374}/D^b$, or Flu $PA_{224–233}/D^b$) and antibodies to cell surface markers (CD8, CD44, CD43 [1B11], CD62L, CD27, CXCR3, CD127, KLRG1, or PD-1). Samples were run on FACSCalibur (BD Biosciences) or CyAn ADP (DakoCytomation) flow cytometers. Data were analyzed using FlowJo software (Tree Star).

Intracellular BrdU staining. BrdU staining was performed as described previously (51). Mice were administered 0.8 mg/ml BrdU in the drinking water for 14 d. Splenocytes were then stained as described above and fixed overnight at 4°C in 1% paraformaldehyde/PBS containing 0.05% Nonidet P-40. After washing, cellular DNA was denatured with DNase I (bovine pancreas; Sigma-Aldrich). Cells were subsequently stained with anti–BrdU-FITC.

Intracellular cytokine and granzyme B staining. Sorted memory $CD8^+$ T cell subsets were co-cultured at 37°C for 5 h with naive $CD45.1^+$ splenocytes pulsed with 1 μg of Sendai $NP_{324–332}$ peptide in 250 μl of CTM containing 10 μg/ml brefeldin A (Epicenter Biotechnologies) and 10 U/ml IL-2 (R&D Systems). After culture, the cells were stained with anti-CD8 and anti-CD45.2 in PBS/brefeldin A. The cells were then fixed in 2% formaldehyde, permeabilized with buffer containing 0.5% saponin, and stained with either anti–IFN-γ, anti–TNF-α, or anti–IL-2 monoclonal antibodies conjugated to APC (BD Biosciences). For granzyme B staining, cells were fixed and permeabilized using the Cytofix/Cytoperm kit (BD Biosciences) after tetramer and surface marker staining. Cells were stained with anti–granzyme B or isotype control antibody conjugated to PE (Caltag Laboratories).

Isolation of memory $CD8^+$ T cell subpopulations by FACS. Lymphocytes were isolated from spleens and further enriched for $CD8^+$ cells using negative selection T cell enrichment columns (R&D Systems). In two-way sorting, enriched $CD8^+$ cells were stained with anti–CD44-FITC and either anti–CD43 (1B11)-PE, anti–CD27-PE, or anti–CXCR3-PE. $CD44^{hi}$ cells were sorted into two subsets based on the expression of the other cell surface marker; e.g., $CD44^{hi}CD43^{hi}$ and $CD44^{hi}CD43^{lo}$. In three-way sorting, enriched $CD8^+$ cells were stained with anti–CD44-APC-AF750 and anti–CD43 (1B11)-AF488 in combination with either anti–CXCR3-PE or anti–CD27-PE. $CD44^{hi}$ cells were sorted into three subsets based on the expression of CD43 and the other cell surface marker; e.g., $CD44^{hi}CD43^{lo}CXCR3^{hi}$, $CD44^{hi}CD43^{lo}CXCR3^{lo}$, and $CD44^{hi}CD43^{hi}CXCR3^{hi}$ (Fig. S1). Sorting was performed on a FACSVantage cell sorter with DIVA enhancement software (BD Biosciences).

Dual adoptive transfer of memory subsets. Dual adoptive transfer experiments were performed as described previously (28, 29). In brief, memory subsets from the donors were combined such that the number of Sendai $NP_{324–332}/K^b$-specific T cells in each donor population was equal. The combined cell subsets were intravenously transferred into naive recipients and then intranasally challenged with 250 EID_{50} of Sendai virus 1 d later. On day 11 after infection, lymphocytes were isolated from various tissues, stained with Sendai $NP_{324–332}/K^b$ tetramer-APC, anti–CD8-PerCP, anti–CD45.1-FITC, and anti–CD90.2-PE, and then analyzed by flow cytometry. The relative response in each tissue was calculated from the numbers of Sendai $NP_{324–332}/K^b$-specific T cells derived from each donor. Control experiments demonstrated that neither anti-CD43 (1B11), anti-CD27, nor anti-CXCR3 monoclonal antibody staining negatively affected the ability of donor cells to mount a recall response in vivo.

Online supplemental material. An example of the sorting strategy used to isolate memory $CD8^+$ T cell subsets for functional studies is shown in Fig. S1, which is available at http://www.jem.org/cgi/content/full/jem.20070322/DC1.

We thank Simon Monard and Brandon Sells for assistance with flow cytometry, the Molecular Biology Core for producing tetramers, and Drs. Marcy Blackman and William Reiley for critically reviewing the manuscript.

This work was supported by National Institutes of Health grants AG021600, AI055500, HL63925, and AI58668, and funds from the Trudeau Institute.

The authors have no conflicting financial interests.

Submitted: 13 February 2007
Accepted: 25 May 2007

REFERENCES

1. Seder, R.A., and R. Ahmed. 2003. Similarities and differences in CD4+ and CD8+ effector and memory T cell generation. *Nat. Immunol.* 4: 835–842.
2. Marshall, D.R., S.J. Turner, G.T. Belz, S. Wingo, S. Andreansky, M.Y. Sangster, J.M. Riberdy, T. Liu, M. Tan, and P.C. Doherty. 2001. Measuring the diaspora for virus-specific CD8+ T cells. *Proc. Natl. Acad. Sci. USA.* 98:6313–6318.
3. Hogan, R.J., E.J. Usherwood, W. Zhong, A.D. Roberts, R.W. Dutton, A.G. Harmsen, and D.L. Woodland. 2001. Activated antigen-specific CD8+ T cells persist in the lungs following recovery from respiratory virus infections. *J. Immunol.* 166:1813–1822.
4. Wiley, J.A., R.J. Hogan, D.L. Woodland, and A.G. Harmsen. 2001. Antigen-specific CD8+ T cells persist in the upper respiratory tract following influenza virus infection. *J. Immunol.* 167:3293–3299.
5. Hogan, R.J., W. Zhong, E.J. Usherwood, T. Cookenham, A.D. Roberts, and D.L. Woodland. 2001. Protection from respiratory virus infections can be mediated by antigen-specific CD4+ T cells that persist in the lungs. *J. Exp. Med.* 193:981–986.
6. Flynn, K.J., G.T. Belz, J.D. Altman, R. Ahmed, D.L. Woodland, and P.C. Doherty. 1998. Virus-specific CD8+ T cells in primary and secondary influenza pneumonia. *Immunity.* 8:683–691.
7. Dutton, R.W., L.M. Bradley, and S.L. Swain. 1998. T cell memory. *Annu. Rev. Immunol.* 16:201–223.
8. Hammarlund, E., M.W. Lewis, S.G. Hansen, L.I. Strelow, J.A. Nelson, G.J. Sexton, J.M. Hanifin, and M.K. Slifka. 2003. Duration of antiviral immunity after smallpox vaccination. *Nat. Med.* 9:1131–1137.
9. Usherwood, E.J., R.J. Hogan, G. Crowther, S.L. Surman, T.L. Hogg, J.D. Altman, and D.L. Woodland. 1999. Functionally heterogeneous CD8+ T-cell memory is induced by Sendai virus infection of mice. *J. Virol.* 73:7278–7286.
10. Murali-Krishna, K., J.D. Altman, M. Suresh, D.J. Sourdive, A.J. Zajac, J.D. Miller, J. Slansky, and R. Ahmed. 1998. Counting antigen-specific CD8 T cells: a reevaluation of bystander activation during viral infection. *Immunity.* 8:177–187.
11. Masopust, D., V. Vezys, A.L. Marzo, and L. Lefrancois. 2001. Preferential localization of effector memory cells in nonlymphoid tissue. *Science.* 291:2413–2417.
12. Reinhardt, R.L., A. Khoruts, R. Merica, T. Zell, and M.K. Jenkins. 2001. Visualizing the generation of memory CD4 T cells in the whole body. *Nature.* 410:101–105.
13. Cauley, L.S., T. Cookenham, T.B. Miller, P.S. Adams, K.M. Vignali, D.A. Vignali, and D.L. Woodland. 2002. Cutting edge: virus-specific CD4+ memory T cells in nonlymphoid tissues express a highly activated phenotype. *J. Immunol.* 169:6655–6658.
14. Sallusto, F., D. Lenig, R. Forster, M. Lipp, and A. Lanzavecchia. 1999. Two subsets of memory T lymphocytes with distinct homing potentials and effector functions. *Nature.* 401:708–712.
15. Lefrancois, L., and D. Masopust. 2002. T cell immunity in lymphoid and non-lymphoid tissues. *Curr. Opin. Immunol.* 14:503–508.
16. Wherry, E.J., V. Teichgraber, T.C. Becker, D. Masopust, S.M. Kaech, R. Antia, U.H. Von Andrian, and R. Ahmed. 2003. Lineage relationship and protective immunity of memory CD8 T cell subsets. *Nat. Immunol.* 3:225–234.
17. Kapasi, Z.F., K. Murali-Krishna, M.L. McRae, and R. Ahmed. 2002. Defective generation but normal maintenance of memory T cells in old mice. *Eur. J. Immunol.* 32:1567–1573.
18. Unsoeld, H., S. Krautwald, D. Voehringer, U. Kunzendorf, and H. Pircher. 2002. Cutting edge: CCR7+ and CCR7- memory T cells do not differ in immediate effector cell function. *J. Immunol.* 169:638–641.
19. Bjorkdahl, O., K.A. Barber, S.J. Brett, M.G. Daly, C. Plumpton, N.A. Elshourbagy, J.P. Tite, and L.L. Thomsen. 2003. Characterization of CC-chemokine receptor 7 expression on murine T cells in lymphoid tissues. *Immunology.* 110:170–179.
20. Hikono, H., J.E. Kohlmeier, K.H. Ely, I. Scott, A.D. Roberts, M.A. Blackman, and D.L. Woodland. 2006. T-cell memory and recall responses to respiratory virus infections. *Immunol. Rev.* 211:119–132.
21. Zanetti, M., and G. Franchini. 2006. T cell memory and protective immunity by vaccination: is more better? *Trends Immunol.* 27:511–517.
22. Vaccari, M., C.J. Trindade, D. Venzon, M. Zanetti, and G. Franchini. 2005. Vaccine-induced CD8+ central memory T cells in protection from simian AIDS. *J. Immunol.* 175:3502–3507.
23. Bachmann, M.F., P. Wolint, K. Schwarz, P. Jager, and A. Oxenius. 2005. Functional properties and lineage relationship of CD8+ T cell subsets identified by expression of IL-7 receptor alpha and CD62L. *J. Immunol.* 175:4686–4696.
24. Marzo, A.L., K.D. Klonowski, A. Le Bon, P. Borrow, D.F. Tough, and L. Lefrancois. 2005. Initial T cell frequency dictates memory CD8+ T cell lineage commitment. *Nat. Immunol.* 6:793–799.
25. Stock, A.T., C.M. Jones, W.R. Heath, and F.R. Carbone. 2006. Cutting edge: central memory T cells do not show accelerated proliferation or tissue infiltration in response to localized herpes simplex virus-1 infection. *J. Immunol.* 177:1411–1415.
26. Berenzon, D., R.J. Schwenk, L. Letellier, M. Guebre-Xabier, J. Williams, and U. Krzych. 2003. Protracted protection to *Plasmodium berghei* malaria is linked to functionally and phenotypically heterogeneous liver memory CD8+ T cells. *J. Immunol.* 171:2024–2034.
27. Klonowski, K.D., A.L. Marzo, K.J. Williams, S.J. Lee, Q.M. Pham, and L. Lefrancois. 2006. CD8 T cell recall responses are regulated by the tissue tropism of the memory cell and pathogen. *J. Immunol.* 177:6738–6746.
28. Roberts, A.D., K.H. Ely, and D.L. Woodland. 2005. Differential contributions of central and effector memory T cells to recall responses. *J. Exp. Med.* 202:123–133.
29. Roberts, A.D., and D.L. Woodland. 2004. Cutting edge: effector memory CD8+ T cells play a prominent role in recall responses to secondary viral infection in the lung. *J. Immunol.* 172:6533–6537.
30. Jones, A.T., B. Federsppiel, L.G. Ellies, M.J. Williams, R. Burgener, V. Duronio, C.A. Smith, F. Takei, and H.J. Ziltener. 1994. Characterization of the activation-associated isoform of CD43 on murine T lymphocytes. *J. Immunol.* 153:3426–3439.
31. Kaech, S.M., J.T. Tan, E.J. Wherry, B.T. Konieczny, C.D. Surh, and R. Ahmed. 2003. Selective expression of the interleukin 7 receptor identifies effector CD8 T cells that give rise to long-lived memory cells. *Nat. Immunol.* 4:1191–1198.
32. Croft, M. 2003. Costimulation of T cells by OX40, 4-1BB, and CD27. *Cytokine Growth Factor Rev.* 14:265–273.
33. Onami, T.M., L.E. Harrington, M.A. Williams, M. Galvan, C.P. Larsen, T.C. Pearson, N. Manjunath, L.G. Baum, B.D. Pearce, and R. Ahmed. 2002. Dynamic regulation of T cell immunity by CD43. *J. Immunol.* 168:6022–6031.
34. Voehringer, D., C. Blaser, P. Brawand, D.H. Raulet, T. Hanke, and H. Pircher. 2001. Viral infections induce abundant numbers of senescent CD8 T cells. *J. Immunol.* 167:4838–4843.
35. Barber, D.L., E.J. Wherry, D. Masopust, B. Zhu, J.P. Allison, A.H. Sharpe, G.J. Freeman, and R. Ahmed. 2006. Restoring function in exhausted CD8 T cells during chronic viral infection. *Nature.* 439:682–687.
36. Zajac, A.J., J.N. Blattman, K. Murali-Krishna, D.J. Sourdive, M. Suresh, J.D. Altman, and R. Ahmed. 1998. Viral immune evasion due to persistence of activated T cells without effector function. *J. Exp. Med.* 188:2205–2213.
37. Tan, J.T., B. Ernst, W.C. Kieper, E. LeRoy, J. Sprent, and C.D. Surh. 2002. Interleukin IL-15 and IL-7 jointly regulate homeostatic proliferation of memory phenotype CD8+ cells but are not required for memory phenotype CD4+ cells. *J. Exp. Med.* 195:1523–1532.
38. Zhang, X., S. Sun, I. Hwang, D.F. Tough, and J. Sprent. 1998. Potent and selective stimulation of memory-phenotype CD8+ T cells in vivo by IL-15. *Immunity.* 8:591–599.
39. Badovinac, V.P., K.A. Messingham, S.E. Hamilton, and J.T. Harty. 2003. Regulation of CD8+ T cells undergoing primary and secondary responses to infection in the same host. *J. Immunol.* 170:4933–4942.
40. Agostini, C., M. Facco, M. Siviero, D. Carollo, S. Galvan, A.M. Cattelan, R. Zambello, L. Trentin, and G. Semenzato. 2000. CXC chemokines IP-10 and mig expression and direct migration of pulmonary CD8+/CXCR3+ T cells in the lungs of patients with HIV infection and T-cell alveolitis. *Am. J. Respir. Crit. Care Med.* 162:1466–1473.
41. Appay, V., P.R. Dunbar, M. Callan, P. Klenerman, G.M. Gillespie, L. Papagno, G.S. Ogg, A. King, F. Lechner, C.A. Spina, et al. 2002. Memory CD8+ T cells vary in differentiation phenotype in different persistent virus infections. *Nat. Med.* 8:379–385.

42. Hendriks, J., Y. Xiao, J.W. Rossen, K.F. van der Sluijs, K. Sugamura, N. Ishii, and J. Borst. 2005. During viral infection of the respiratory tract, CD27, 4-1BB, and OX40 collectively determine formation of CD8+ memory T cells and their capacity for secondary expansion. *J. Immunol.* 175:1665–1676.
43. Borst, J., J. Hendriks, and Y. Xiao. 2005. CD27 and CD70 in T cell and B cell activation. *Curr. Opin. Immunol.* 17:275–281.
44. Hamann, D., P.A. Baars, M.H. Rep, B. Hooibrink, S.R. Kerkhof-Garde, M.R. Klein, and R.A. van Lier. 1997. Phenotypic and functional separation of memory and effector human $CD8^+$ T cells. *J. Exp. Med.* 186:1407–1418.
45. Ellies, L.G., A.T. Jones, M.J. Williams, and H.J. Ziltener. 1994. Differential regulation of CD43 glycoforms on CD4+ and CD8+ T lymphocytes in graft-versus-host disease. *Glycobiology*. 4:885–893.
46. He, Y.W., and M.J. Bevan. 1999. High level expression of CD43 inhibits T cell receptor/CD3-mediated apoptosis. *J. Exp. Med.* 190:1903–1908.
47. Matsumoto, M., K. Atarashi, E. Umemoto, Y. Furukawa, A. Shigeta, M. Miyasaka, and T. Hirata. 2005. CD43 functions as a ligand for E-Selectin on activated T cells. *J. Immunol.* 175:8042–8050.
48. Stockton, B.M., G. Cheng, N. Manjunath, B. Ardman, and U.H. von Andrian. 1998. Negative regulation of T cell homing by CD43. *Immunity*. 8:373–381.
49. D'Souza, W.N., and S.M. Hedrick. 2006. Cutting edge: latecomer CD8 T cells are imprinted with a unique differentiation program. *J. Immunol.* 177:777–781.
50. Cole, G.A., T.L. Hogg, and D.L. Woodland. 1994. The MHC class I-restricted T cell response to Sendai virus infection in C57BL/6 mice: a single immunodominant epitope elicits an extremely diverse repertoire of T cells. *Int. Immunol.* 6:1767–1775.
51. Cauley, L., T. Cookenham, R. Hogan, S. Crowe, and D. Woodland. 2003. Renewal of peripheral CD8 memory T cells during secondary viral infection of antibody sufficient mice. *J. Immunol.* 170:5597–5606.